ASIM: An analytic PET simulator

Brian Elston, Claude Comtat, Robert Harrison, and Paul Kinahan

Brian Elston: Department of Radiology, University of Washington, Seattle, U.S.A.
Claude Comtat: CEA, SHFJ, Orsay, F-91401, France
Robert Harrison: Department of Radiology, University of Washington, Seattle, U.S.A.
Paul Kinahan: Department of Radiology, University of Washington, Seattle, U.S.A.

A. Outline

1. Introduction
2. Role of simulation in PET research
3. Analytic PET simulation
4. Development and history of ASIM
5. Structure of ASIM
6. Algorithmic description of the analytic simulator
7. Usage illustration
8. Example studies using ASIM
9. Future direction

1. Introduction

Simulation plays an important role in the development of positron emission tomography (PET). It is used extensively in the design of tomographs, in the investigation of physical effects that cannot be quantified using experiments, in the development of data correction and image reconstruction algorithms, and in the development of imaging protocols. Historically simulation led to understanding the effect of scatter on PET images, the design of septa, the effects of noise on PET images, and the sensitivity and resolution limits of PET. Simulation continues to be used in these areas for PET and all other image modalities ([Lewellen 1998], [Comtat 1999], [Buvat 2002]).

In positron emission tomography patient scans the true underlying activity distribution is unknown. We have no way of knowing in a given scan how various factors are confounding the data; statistical noise, biological variability, scattered radiation, patient motion, deadtime in the detectors and electronics, detector resolution and partial volume, septal penetration, and random coincidences. Simulation provides an unparalleled window for examining these factors [Ljungberg 1998]; they can be designed to isolate a single factor of interest, for instance when researchers perform multiple simulations of the same imaging situation to determine the effect of statistical noise or biological variability. Simulations are also increasingly used as a design tool for commercial tomographic scanners.

2. Role of simulation in PET research

The wide range of problems being addressed has lead to a tremendous variety of tools. The most exact simulations are the particle-tracking variety used for high-energy physics simulations, for example Géant [GEANT], EGS [EGS], MCNP [MCNP], and Penelope ([PENELOPE2005], [Sempau 2003]). These cover the full range of possible interactions and allow for very detailed descriptions of tomographs and imaged objects. Their drawbacks are that they are slow and can be difficult to set up for medical imaging simulations. Efforts have been made to simplify their use for medical imaging, notably the Geant4 Application for Tomographic Emission (GATE) [GATE] and PET-EGS ([PET-EGS], [Castiglioni 1999]). With proper set-up, the high-energy physics packages can provide very accurate simulations. A complete simulation is still, however, painstakingly slow. A whole body PET scan can take days, weeks, months or more to simulate on a modern single processor computer.

There are also general use photon-tracking simulations that are tailored specifically for medical imaging, for example SimSET [Lewellen 1998] for PET and SPECT, PETSIM [Thompson 1992] for PET, and SIMIND ([SIMIND], [Ljungberg 1989]) for SPECT. These packages support more limited, tomograph-specific geometries and concentrate on tracking photons within a limited energy range, reducing the types of interactions that must be simulated. These simulations are easier to set-up and faster than the high-energy physics packages. The restrictions on geometries make it difficult or impossible to use these packages to simulate some innovative new ideas (e.g. [Tai 2006]) and limitations on the particles simulated make these packages less exact than the high-energy applications. However, their accuracy is usually satisfactory for comparative

design studies, for characterizing the contaminants in data and assessing the relative importance of various contaminants, and for examining the impact of data correction methods (e.g. scatter correction).

Scattered radiation has been one of the areas most studied with simulation (e.g., [Bai 2000], [Barret 2005], [Haynor 1995]) and has produced some single purpose photon-tracking simulations, for example those of Holdsworth [Holdsworth 2002] and Beekman [Beekman 1997]. These packages are less flexible, both in their modeled geometry and modeled physics, than the general packages above. However, for the single purpose of estimating scatter distribution they are considerably faster than the other packages. This allows for the investigation of patient specific scatter elimination. The simplest model is Line of Response (LOR) coincidence generation (i.e. Sim3D [Sim3D 1994], PETTRACE) which directly generate true coincidence events.

The time required for a photon-tracking simulation varies linearly with the number of decays (typically many billions) simulated. Although photon-tracking simulations are amenable to parallelization and/or importance sampling, this does not provide the acceleration necessary for studies requiring many realistic simulations. These kinds of applications are the motivation for providing even faster simulation methods.

3. Analytic PET simulation

Simulations that require sufficient photons for multiple image formations are in general a challenge for photon-tracking simulations. An example of this type of study are those aimed at understanding and optimizing patient PET imaging. In particular, observer studies of tumor detectability, image noise measurements, and kinetic modeling studies often require hundreds or thousands of realizations of a small set of imaging configurations.

Multiple realizations can be more quickly produced using analytic simulations ([Furuie 1994], [Comtat 1999]). An analytic simulation calculates mean estimates of each sinogram bin based on a ray-tracing model. These mean values can then be used as noiseless data, or a noisy data set can be produced by adding noise to each data value; done correctly this is a form of bootstrapping [Haynor 1989]. As the addition of noise to a data set such as a sinogram takes virtually no time with modern computers, analytic simulations are often used in situations where multiple noisy realizations of the same data are required. Unfortunately many data contaminants are difficult to model in a general and accurate way (for if they were easy to model they would be easy to correct). Analytic simulations must rely on simplified models or object and tomograph-specific models for these contaminants (for instance derived from a photon-tracking simulation like SimSET). However, image reconstructions of data from analytic simulations can give quite accurate approximations of noise and resolution properties.

The tradeoffs that analytic simulators make in comparison with the more accurate photon tracking simulations are that all effects (noise, scatter, randoms, attenuation, etc.) are calculated rather than naturally arising out of following the fate of individual photons. Most of the important effects such as noise, attenuation, and detector blurring can be accurately calculated, but not scatter. Without photon tracking, scatter can only be roughly estimated in PET scanners or in tractable simulations. Thus, we can reliably estimate the noise added by scatter (at least relative to other sources of noise), but not the bias. In practice the bias from scatter is imperfectly estimated ([Wollenweber 2002], [Watson 2000], [Ollinger 1996]) thus leaving a residual bias after scatter correction. The analytical simulator ASIM [Comtat 1999] does not attempt to estimate this residual due to the challenge of using an appropriate model for the residual bias. Instead the mean estimated scatter is used first to calculate the added noise due to scatter and then used for scatter correction, leaving no residual bias. The scatter is either predetermined (e.g. from measurements or photon tracking simulations) or estimated using the Klein-Nishina equation, using a simplified representation of the object to reduce computation time.

Some researchers have adopted directly adding noise to images or image-derived data for kinetic modeling (e.g. [Marcinkowski 2005], [Alpert 2003]). These simulations are very fast, but have the disadvantage of being prone to bias and other inaccuracies. They are often used when researchers desire a quick way to generate data and find there are no public domain or open source tools appropriate for their task (e.g. [Lahorte 2000], [Ward 2005]). However, if instead the mean of the acquired data is estimated, and the estimated mean values replaced with Poisson-distributed random variables about the means, a new Poisson-distributed random variable is generated. Thus new realizations can be very quickly generated once the mean values are estimated. A tradeoff of image based analytic simulations is that noise correlation effects are not included. These effects are often a dominant factor in real images.

The strength of analytic simulations is that while the first noiseless data set can require extensive computation, noisy realizations can be generated very quickly by adding noise. Thus generating hundreds or thousands of realizations requires little more time than one realization, making analytic simulation methods a good choice when many noisy Independent Identically Distributed (i.i.d.) realizations of the same configuration are needed. This often occurs, for example, in the quantitative assessment of image quality (e.g. [Lartizien 2004]). As described above, a trade-off is that analytics simulation methods cannot, by themselves, accurately simulate such data contaminants as scatter, random coincidences, pulse pileup, or detector blurring. These physical effects must be estimated by other means, such as phantom scans or photon-tracking simulations, which is a potential source of bias. Analytic simulators have been developed for SPECT ([Lahorte 2000], [Ward 2005]) and for PET ([Rowe 1992], [Furuie 1994], [Comtat 1999]).

From analytic simulation methods to photon tracking methods, Table 1 summarizes the advantages of the various simulation packages discussed above. In general, flexibility and accuracy come at the cost of speed and ease-of-use. The hybrid packages, GATE and PET-EGS, trade some of the flexibility of the high-energy physics simulations for ease-of-use similar to the general purpose photon-tracking simulations, while retaining the accuracy advantage and speed disadvantage of their underlying high-energy simulations.

Table 1: The major simulation packages can be arranged by increasing flexibility and accuracy/decreasing speed. A more comprehensive comparison (without analytic simulations) can be found in “Monte Carlo simulations in SPECT and PET” [Buvat 2002].

Tradeoff	More accurate (slower) ⟷ More precise (faster)						
Mode	Photon-tracking					Analytic	
Role	High energy physics (HEP)	Adapted HEP	General purpose nuclear medicine	Special purpose nuclear medicine	True coincidence only	Sinogram based	Image based
Instances	Geant, EGS4, MNCP	GATE	SimSET, SIMIND, PET-EGS, PETSIM	Beekman, Holdsworth	Sim3D, PETTRACE	ASIM	Alpert
Pros	Most accurate and flexible. Carefully validated. Freely available.	Accurate and flexible. Freely available.	Accurate and faster than HEP based methods. Freely available.	Faster than general purpose medical.	Fastest photon-tracking method. Relatively simple. Useful for debugging and testing reconstruction algorithms.	Much faster than photon-tracking methods. Can include important physics effects. Some are freely available.	Fastest, simplest method.
Cons	Very slow and complex to setup and run.	Slow, somewhat complex.	Less flexible, less accurate than HEP based methods.	Only specific interactions (e.g. Compton scatter). Inflexible and less accurate than general purpose packages. No independent validation.	Does not model important effects (e.g. attenuation, scatter, randoms).	Some physics effects (e.g. scatter) must be approximated.	Does not model physics or noise correlations in images. No independent validation.

[GEANT 1999], [EGS 1985], [MCNP], [GATE 2004], (SimSET) [Lewellen 1998], (SIMIND) [Ljungberg 1989], (PET- EGS) [Castiglioni 1999], (PETSIM) [Thompson 1992], [Beekman 1997], [Holdsworth 2002], [Sim3D 1994], [PETTRACE], (ASIM) [Comtat 1999], [Alpert 2003].

4. Development and history of ASIM

The analytic simulator (ASIM) was developed under NIH funding (R29-CA74135: PI Kinahan, "Strategies for Clinical Oncology Imaging with 3DPET") starting in 1997 and continuing through today by a collaborative work between the SHFJ in Orsay, France, and the University of Washington (R01-CA115870, R01-CA126593, R01-CA42593, and U01-CA148131) in Seattle, U.S.A.

In 1996 Michel Defrise and Christian Michel designed and coded the original version (1.0) of the ASIM analytic simulator with a low-level, but fast, Poisson noise generator. In 1997 Claude

Comtat and Paul Kinahan expanded on the project, creating version 3.0, which progressed to version 5.52 by March 2011 with many new additions to the physics model. These versions are coupled to the CTI PET scanner geometry via the ECAT software library of M. Sibomana and C. Michel. In 2008 Brian Elston and Paul Kinahan created from ASIM 5.39 a version with scanner independent Input-Output (I/O), available publicly as an open source project since 2010 at http://depts.washington.edu/asimuw/.

Researchers have utilized the ASIM simulation package to study lesion detectability in response to reconstruction techniques ([Lartizien 2003], [Janeiro 2006]), scan duration [Cheng 2004] and weight based scanning protocol [Kinahan 2005] in positron emission tomography (PET) oncology imaging. These studies utilized multiple independent realizations to quantify numerically the detectability of various sized lesions simulated within an extended MCAT phantom in an emulated ECAT HR+ scanner [Lartizien 2003]. More recent studies have examined the detectability of patient response to therapy as a result of tumor change between PET scans using common evaluation techniques (for example contrasting PERCIST and EORTC) [Harrison 2010]; and the effects of noise, calibration, reconstruction, and analysis methods on correctly determining change in PET SUVs through simulation studies [Kinahan 2011]. The code was also used to simulate dynamic PET studies and evaluate pharmacokinetic measurements [Maroy 2008]. There are examples of images reconstructed from ASIM simulation data at the end of this chapter.

5. Structure of ASIM

ASIM is a software toolkit designed as a fast analytic simulator for positron emission scanners. The package provides a variety of options including the simulation of emission data, attenuation correction, randoms, scatter, detector efficiencies, 2D and 3D mode, detector blurring, normalization, and noise propagation. The scanner independent Input-Output (I/O) is supported with the YAFF format (Yet Another File Format), which is based on the interfile model of two output files, one an ASCII header and the other a sinogram data block. The extension used for the data block is .yaff, and .yhdr is used for the header file in the YAFF format.

The header file contains parameters relevant to the description of the simulation data block. The sinogram data block is comprised of 4 dimensional projection data (radial, azimuthal, axial, and ring difference) in big-endian 4-byte floating point format. The software is coded in ANSI compliant C, using modern software architecture and coding practices, tested and compiled under UNIX using a Macintosh system. The code is hierarchically organized in a functionally derived C style, so as to be easily modifiable, expandable, and debuggable.

There are three core modules of the ASIM software package:

Simul:	Generates noiseless PET emission and attenuation sinograms.
Noise:	Applies Poisson-distributed noise to a sinogram.
Normalize:	Applies corrections to these data sets.

The three modules are run in series for investigative studies, in conjunction with reconstruction and analysis, creating a chain of software simulation command calls with parameters which can be automated through a shell script to create multiple realizations easily as diagramed in Figure 1.

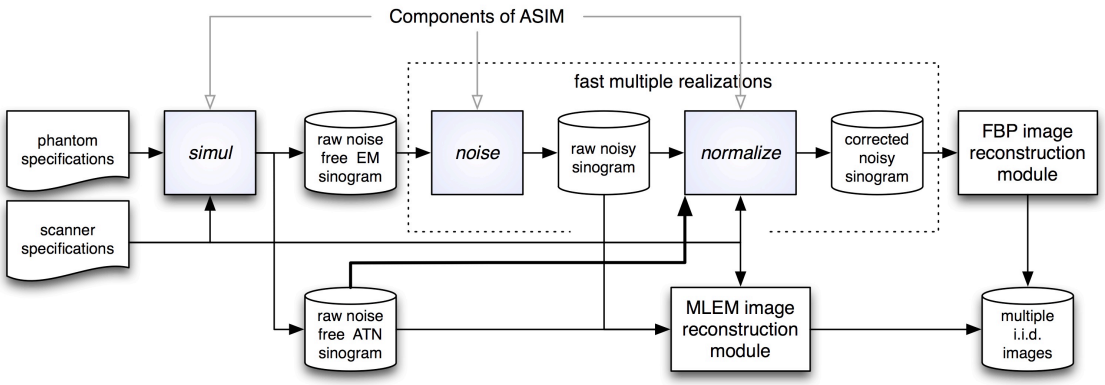

Figure 1: Typical procedural flow using Simul, Noise, and Normalize to generate multiple realizations for an example study. Here one (or potentially more) raw noise-free EM (emission) sinograms are created along with a raw noise-free ATN (attenuation) sinogram. Image reconstruction is performed with filtered-backprojection (FBP) or Maximum-Likelihood Expectation-Maximization (MLEM) to obtain multiple independent identically distributed (i.i.d.) images. (From ASIM website. With permission.)

In Simul, phantoms can be specified as collections of geometric solids and noiseless line-integrals through these phantoms are calculated. The calculations are performed analytically, not numerically, to avoid any interactions with iterative image reconstruction methods that use numerically calculated system matrices. Alternatively, pixelized phantoms can be provided; line-integrations are then calculated numerically. Once the noise-free sinogram data is generated, multiple independent noisy realizations can be quickly generated. By separately generating noise-free sinograms of lesions, composite sinograms can be created with varying contrast and noise levels. Attenuation, scatter, randoms, detector efficiencies, and isotope decay are used to calculate the Poisson random deviates for each sinogram element. The count levels for the simulations are set either explicitly by specifying the number of true, scattered, and random coincidences for a given bed position (whole-body scans) or temporal frame (dynamic scans), or implicitly by specifying a unique calibration factor for true and random coincidences, plus a scatter fraction. Given the isotope half-life and the emission and transmission scan durations, count levels are calculated for each bed position and temporal frame. The sinograms are processed and reconstructed with the same procedures used with measured data to ensure the same correlated noise properties in the reconstructed images.

Corrections that can be applied by Normalize include attenuation correction, axial normalization, random and scattered coincidences correction, and arc correction, among others.

Prior validation studies with ASIM created a generic extended MCAT phantom, written by C. Lartzien, using the geometric phantom scripting system provided within the software [Lartizien 2003], as can be seen in Figure 2. Here a collection of truncated ellipsoids (including variations such as cylinders) were used to represent a generic human form. Of note in the emission image we can clearly identify the heart, brain, arms, spine, lungs, bladder, stomach, liver, kidneys, and spleen. Identifiable in the attenuation image are the skull, lungs, ribs, arm bones (humerus, ulna, radius), and spine.

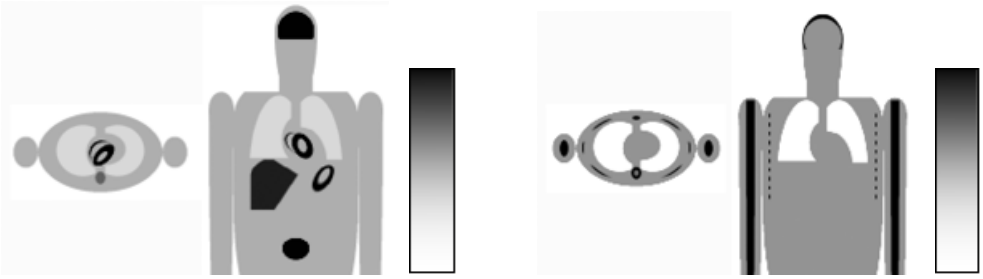

Figure 2: *Emission density (left) in e[counts/mm] and linear attenuation coefficient in u[1/mm], simulated with ASIM.*

Several extensions have been added over the years to improve the accuracy of the simulation. Most notably it is now possible to include a model of the spatially-dependent resolution in a clinical PET scanner.

6. Algorithmic description of the analytic simulator

For geometrical phantoms, true coincidences, for both emission and transmission, are determined by analytic projection along Line of Response's (LORs) through the emission and attenuation objects. This method was chosen as it does not require projecting a pixelized image of the phantom, thus avoiding numerical integration and the computational resources required by those methods. It is also possible to input a pixelized phantom image, in particular useful for brain imaging simulations. Effects of attenuation, normalization, and blank scan are included in the calculation of true coincidences. These calculated projections are blurred by a 2D smoothing filter in the radial and axial directions to reflect the intrinsic spatial resolution of the scanner.

In a scan simulation three types of events can be detected; true, random, and scattered coincidences. It is assumed that the portion of scattered coincidences in the transmission scan is insignificant, and that the transmission scan is not contaminated by emissions from phantom activity. Poisson noise is contributed from four sources in PET; the emission, transmission, normalization, and blank scans; however ASIM assumes no significant noise is contributed by the normalization and blank scans.

As a result five independent Poisson noise sources are considered; emission trues, emission randoms, emission scatter, transmission trues, and transmission random coincidences. These five sinogram elements are specified by the bed position, temporal frame, and Line of Response (LOR); parameterized by the radial position, azimuthal angle, mid-slice axial position, and the ring difference. The data composing these five noiseless sinogram elements are determined from the phantom geometry, scanner geometry, the bed position, temporal framing for dynamic acquisition and multi-bed acquisition, the number of bed positions, and their overlap.

The phantom geometry is specified by a collection of 3D geometric shapes, each an ellipsoid object. Each object is assigned an emission density and attenuation coefficient. Within a given object, the emission density follows one of three distributions; uniform, uniform with a linear gradient, or having a radial dependency from the centroid of the ellipsoid. The linear attenuation coefficient within each object is uniform. The units of the emission density can be considered as arbitrary, and thus the simulation does not predict the total numbers of coincidences. These numbers have to be input by the user of the simulation. Alternatively, the units are in Bq per ml, and the simulation predicts the total number of coincidences as long as a calibration factor is specified. This factor depends on the scanner model only and is valid regardless of the simulated phantom.

Scattered or random coincidences are not simulated accurately in ASIM, but rather their effects on sinogram statistics. Since the simulator uses a non Monte-Carlo technique, exact calculation

of randoms and scatter is impossible. Instead a model is used where the total activity in each slice is concentrated along the axis of the scanner, taking into account the activity outside the field of view. While this results in only a rough approximation, it is acceptable as the simulation data is corrected for scatter and randoms assuming no bias. It is only the influence of randoms and scatter on the noise that is relevant given this model, thus not requiring extreme accuracy [Comtat 1999].

7. Usage illustration

For this usage example we will generate two emission sinograms, one for the torso and another for the tumor, as well as an attenuation and normalization scan. We then sum the two emission sinograms, applying a multiplicative factor to one (i.e. the tumor), and add noise to the composite sinogram. This sinogram is then normalized, applying attenuation correction and axial normalization. Lastly we reconstruct the sinogram data into image data, and display it. We generated the following example running the simulation software from the command line parameters shown in Table 2, in the order of execution denoted by process. We used Unix on a Macintosh computer, but the software can run with no or minor modifications on most Unix/Linux and Windows systems.

A Simul emission sinogram was generated with arc effect and Line Of Response Solid Angle Scaling (LORSAS) turned off. We modeled a simplified 3 ring scanner based on the ECAT HR+. We placed the phantom so that the top of the tomograph field-of-view axially was a point 365 mm from the top of the phantom (see the command process 1 in Table 2). In Table 3 we see the command line parameters used for Simul in the usage illustration here. Note that for this example the file named '301' contains the appropriate definitions for the ECAT HR+ scanner (i.e. a scanner definition file), with the number of rings set to three, and the torso.data input file is a Simul phantom representation of an extended MCAT phantom. The torso data output file was named torso_em.yaff, with the header file name defaulting to torso_em.yhdr as a convention. The simulation run was specified to also output scatter and delayed data, as well as specifying a 2D scan with a ring difference of 1. The tumor emission sinogram was generated using the command seen in Table 2 process (2). The tumor input file is tumor.data, and represents a 3 cm diameter lesion in the chest wall. Other parameters generating the tumor emission sinogram are identical to that for generating the emission sinogram for the torso.

Table 2: *Command line parameters, in order of execution, for generating the composite noisy, and subsequently corrected sinograms, that were then reconstructed into the images displayed in Figure 3. (From ASIM website. With permission.)*

Process	Command Line	Effect
(1)	*Simul -i torso.data -o torso_em.yaff -E -k -h -S -D -f 365 -m 301 -d 1*	Generate emission sinogram for torso.
(2)	*Simul -i tumor.data -o tumor_em.yaff -E -k -h -S -D -f 365 -m 301 -d 1*	Generate emission sinogram for tumor.
(3)	*Simul -i torso.data -o torso_atten.yaff -A -k -h -f 365 -m 301 -d 1*	Generate attenuation sinogram for torso.
(4)	*Simul -i torso.data -o torso_norm.yaff -N -k -h -f 365 -m 301 -d 1*	Generate normalization sinogram for torso.
(5)	*Noise -i torso_em.yaff -t 6000000 -r 6000000 -R -s 2100000 -S -J 2.0 -I tumor_em.yaff –o torso_tumor_noisy.yaff*	Sum torso and tumor sinogram, apply multiplicative factor to tumor sinogram, and apply noise to composite sinogram.
(6)	*Normalize -i torso_tumor_noisy.yaff -a torso_atten.yaff -n torso_norm.yaff –k –o torso_tumor_normalized.yaff*	Apply attenuation correction and axial normalization to input sinogram.

Table 3: *Command line parameters and their description used with Simul in the usage illustration. (From ASIM website. With permission.)*

Parameter	Effect
-E	Generate noise-free emission sinogram.
-A	Generate attenuation sinogram.
-N	Generate normalization sinogram.
-S	Generate scatter sinogram.
-D	Generate delayed sinogram.
-i	Select filename for input file (geometric phantom or pixelized).
-o	Select filename for output file (and by convention sets header filename).
-k	Simulate arc effect.
-h	Turn Line Of Response Solid Angle Scaling (LORSAS) off.
-f	Set start of bed position in mm.
-m	Select file that the scanner definition is located in.
-d	Sets the scan dimension to 2D, or 3D.

An attenuation sinogram was generated from the torso with arc effect and LORSAS turned off, using the same 3 ring emulated ECAT HR+ scanner, and starting from the same bed position (Table 2, process 3). The input file to the attenuation simulation is the torso phantom file, torso.data. The input and output filename conventions are the same as that used for the emission sinogram, including the convention for naming header files. All other parameters in the command perform the same as those described above.

A normalization scan was created using the same methodology and process as for the attenuation and emission data (Table 2, process 4).

Noise was added by specifying the number of true counts, in this case 60 million, with random and scatter correction applied, and counts specified representing a typical clinical noise level for randoms and scatter (Table 2, process 5). A description of the command line parameters used with Noise can be seen in Table 4. The primary input file is torso_em.yaff, with the output data block filename, torso_tumor_noisy.yaff, and the output header filename torso_tumor_noisy.yhdr. Additionally the noise application has the ability to sum two sinograms and apply a multiplicative factor to one of them. The additional input sinogram is tumor_em.yaff, and the multiplicative factor specified for it is a value of 2.0. In this study the additional input file was used to model a tumor with varying activity levels within a torso to investigate lesion detectability.

Table 4: *Command line parameters and their description used with Noise in the usage illustration. (From ASIM website. With permission.)*

Parameter	Effect
-S	Apply scatter correction.
-R	Apply random correction.
-i	Select filename for input sinogram file.
-o	Select filename for output file (and by convention sets header filename).
-I	Select filename for secondary optional input sinogram file.
-J	Set multiplicative factor for apply to additional input sinogram from –I command.
-t	Set number of coincidences for true count.
-r	Set number of coincidences for random count.
-s	Set number of coincidences for scatter count.

This noisy emission sinogram was then axially normalized and attenuation corrected (Table 2 process 6). The input file is attenuation corrected using the attenuation sinogram torso_atten.yaff, axially normalized using torso_norm.yaff, with arc correction disabled. In this case arc correction

was disabled as that factor was accounted for in the reconstruction process. In Table 5 we see a description of the command line parameters used with Normalize in this example. The input file is torso_tumor_noisy.yaff, the output sinogram file name is torso_tumor_normalized.yaff, with the header output filename defaulting to torso_tumor_normalized.yhdr.

Table 5: *Command line parameters and their description used with Normalize in the usage illustration. (From ASIM website. With permission.)*

Parameter	Effect
-i	Select filename for input sinogram file.
-o	Select filename for output file (and by convention sets header filename).
-a	Selects input attenuation sinogram and applies attenuation correction.
-n	Selects input normalization sinogram and applies axial normalization.
-k	Arc correction.

The sinogram data was then reconstructed using the filtered-back projection (FBP) implementation FBP2D in the Software for Tomographic Image Reconstruction (STIR [STIR]) library, and STIR's Ordered Subset Maximum A Posteriori One-Step Late (OSMAPOSL) iterative algorithm, and subsequently analyzed. This process can quickly be repeated many times, creating multiple realizations, with individual instantiations having unique noise characteristics. Examples of these images can be seen below in Figure 3.

8. Example studies using ASIM

The study “SNR Effects in Determining Change in PET SUVs in Response to Therapy” [Harrison 2010] conducted an investigation of the relative impact of photon noise and other noise on the ability of PET to detect a response to therapy. ASIM was used to simulate an anthropomorphic phantom with a 3 cm diameter breast tumor in a 3 detector ring tomograph loosely emulating the ECAT HR+, shown in Figure 3. Reconstruction was performed with FBP using a Hann filter cutoff at .5 of the Nyquist frequency, while the OSMAPOSL reconstruction was run 2 iterations, 12 subsets, with a 3 mm Metz filter. An estimate of the Standard Uptake Value (SUV) was obtained using SUV mean and SUV max. Other (non-photon-counting) noise, such as calibration errors and biological variability was estimated by adding varying amounts of Gaussian noise to the SUV estimate. Receiver Operating Characteristics (ROC) curves were created, Area Under the Curve (AUC) was determined, and finally the percentage of realizations that satisfy the European Organization for Research and Treatment of Cancer (EORTC) [EORTC 2011] and PET Response Criteria in Solid Tumors (PERCIST) [Siemens Healthcare Molecular Imaging, 2010] criteria were calculated for partial metabolic response or progressive metabolic disease.

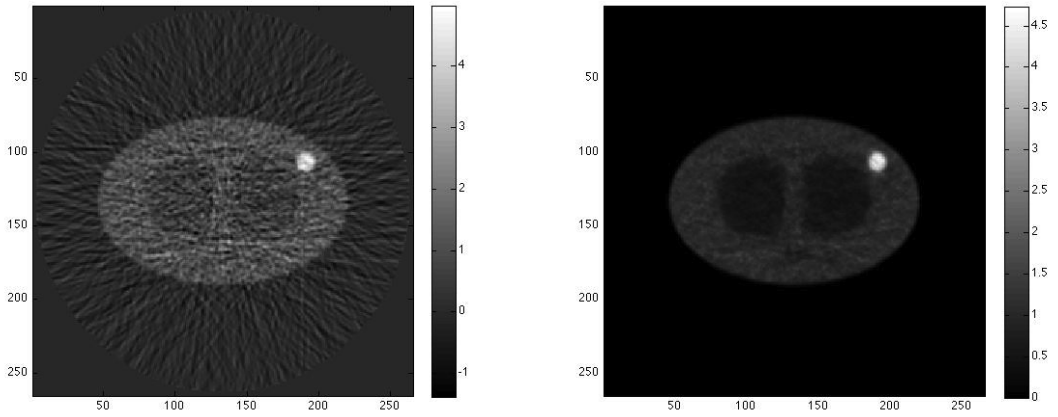

Figure 3: *Filtered backprojection (left) and OSMAPOSL image reconstructions of typical count*

simulations for tumor SUV=2. Sinograms simulated using ASIM, and images reconstructed with STIR.

This investigation concluded that results were much less sensitive to change in scan duration and reconstruction method in comparison to changes in scanner calibration or patient test-retest variability. The PERCIST classification scheme was deemed noticeably less error prone than the EORTC system, misclassifying metabolic response as progression, and vice-versa, less often. EORTC was deemed as having criteria that seemed too narrow, or finely grained, given the current typical system measurement errors.

In Figure 4 we see a study comparison of simulated and measured data, on left measured data from a Siemens/CTI ECAT HR+ scanner acquired in fully-3D mode, and on right simulated data for the same acquisition properties using ASIM.

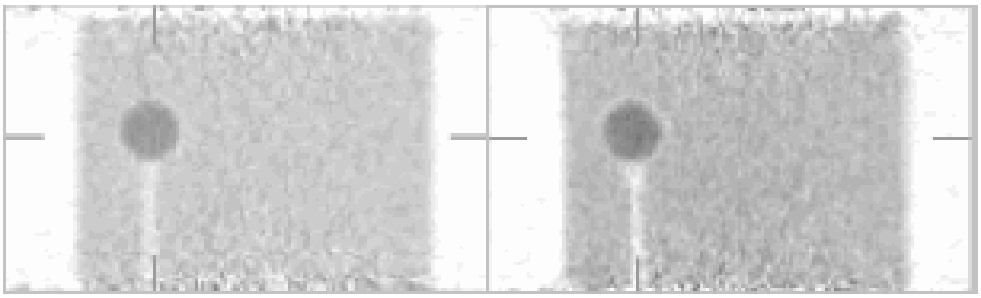

Figure 4: *Transverse orthogonal sections through a 20 cm diameter cylindrical phantom. Left: Measured data from a Siemens/CTI ECAT HR+ scanner. Right: Simulated data for the same acquisition using ASIM. (The vertical streak in the images is the support rod for the hot sphere). (With permission.)*

An examination of how scan duration affects the detectability of tumor masses was performed in the study “A quantitative approach to a weight-based scanning protocol for PET oncology imaging” [Kinahan 2005]. The focus of this study was to investigate the effects of patient attenuation, determined by patient thickness. As attenuation increases the number of photons detected exponentially decreases, thus affecting tumor detectability in PET imaging. The simulation study was performed using an MCAT phantom, with the addition of 18 lesions ranging in size from 1 cm to 3 cm in diameter spaced throughout the phantom, seen in Figure 5. The simulation was performed using ASIM, corrected for attenuation and detector geometry, and reconstructed using Attenuation Weighted Ordered Subset Expectation Maximization (AWOSEM). Detectability for each lesion’s location, size, contrast ratio, and duration was evaluated using a non-pre-whitening matched filter (NPWMF).

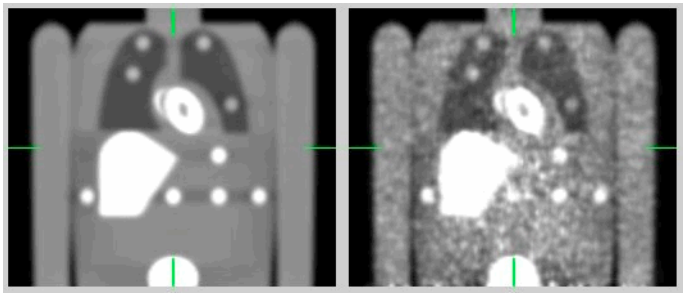

Figure 5: *Coronal slices for image volumes generated by ASIM. Left, noise free reconstruction with 3 cm diameter targets. Right, noisy realization simulating a 5 minute scan.*

This study found that target detectability varies non-linearly with target diameter, as a function of scan duration. Target detectability squared was found to be approximately proportional to scan duration and Noise Equivalent Count (NEC) count density. Notably, while under current clinical practice scan time is typically not adjusted for body habitus, the research found that image quality within the thorax and abdomen degrades with increased body girth.

An investigation of using simulation to predict the progression of tumor growth was conducted in the study “Applying A Patient-Specific Bio-Mathematical Model of Glioma Growth to Develop Virtual [18F]-FMISO PET Images” [Gu 2011]. The study sought to assess the proliferation and invasion of glioma through mathematical modeling. This research used a pharmacokinetic model to determine the activity of a [18F]-flouromisonidazole (FMISO) tracer within the brain over the time interval of virtual PET imaging. This summed tracer map was then processed by ASIM, using a pixelized input phantom, creating a simulated FMISO-PET image that mimics the noise characteristics and acquisition artifacts seen in clinical FMISO-PET images for the patient.

We see in Figure 6 measured and simulated images of MRI and PET images of hypoxic glioma tumor cells. The underlying PET data used for the simulated image is based on a model combining glioma cellular distribution with the pharmacokinetics for FMISO uptake. The model is run forward in time until the glioma volume matches the measured tumor volume (but not necessarily the pattern of distribution) from the patient MRI. Simulated PET images were then generated with ASIM.

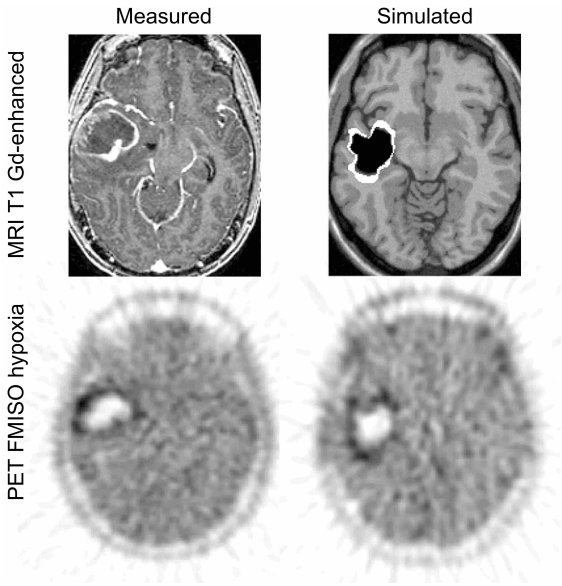

Figure 6: *Measured and simulated images of MRI and PET images of hypoxic glioma tumor cells [Gu 2011].*

This work establishes a direct link between anatomical (MRI) modeling and molecular (PET) imaging and provides a tool for predicting hypoxic distribution on a patient specific level. It demonstrates capabilities of the Proliferation-Invasion-Hypoxia-Necrosis-Angiogenesis (PIHNA) model to produce predictive, patient-specific realizations as visualized on clinical MRI.

9. Future directions

We are currently preparing the first open source release of the ASIM software. The source code has been re-structured and architected into modular function based software using the C programming language. Documentation is being written to describe the simulation package and its usage. The source code and preliminary documentation are presently available online.

Some researchers have indicated that having a simulation meta-language interpreter would be valuable. Currently the inputs and outputs of various simulators, such as ASIM and SimSET, are quite different. Having a common input meta-language, for example describing phantoms and scanner geometries, would make it much easier for users to use multiple simulation packages.

Investigators have expressed desire in a phantom building application that would display the object graphically, and allow for interactive creation of the phantom. ASIM's current system of phantom definition is text based; graphical display would provide the researcher with direct visual feedback when building new phantoms and ease the creation process. The tool would be designed to directly output ASIM compatible phantom definition files, and possibly phantoms compatible with a limited set of other simulation packages.

Acknowledgements

Research supported by NIH grants R01-CA115870, R01-CA126593, R01-CA42593 and U01-CA148131, French ANR grant ANR-05-MMSA-014-01.

References

Alpert, N. M., Rajendra, D., Badgaiyan, Elijahu, L., & Fischman, A. J. (2003). A novel method for noninvasive detection of neuromodulatory changes in specific neurotransmitter systems.

NeuroImage, *vol. 19*, 1049-1060.

ASIM: Analytic PET simulator Home Page (Online). University of Washington.,From: http://depts.washington.edu/asimuw/, (2011).

Bai, C. Y., Zeng, G. S. L., & Gullberg, G. T. (2000). A slice-by-slice blurring model and kernel evaluation using the Klein-Nishina formula for 3D scatter compensation in parallel and converging beam SPECT. *Phys. Med. Biol.*, *vol. 45*(5), 75-1307.

Barret, O., Carpenter, T. A., Clark, J. C., Ansorge, R. E., & Fryer, T. D. (2005). Monte Carlo simulation and scatter correction of the GE advance PET scanner with SimSET and Geant4. *Phys. Med. Biol.*, *vol. 50*, 4823-4840.

Beekman, F. J., Den Harder, J. M., Viergever, M. A., & Van Rijk, P. P. (1997). SPECT scatter modeling in nonuniform attenuating objects. *Phys. Med. Biol.*, *vol. 42*, 1133–1142.

Buvat, I., & Castiglioni, I. (2002). Monte Carlo simulations in SPECT and PET. *J. Nucl. Med.*, *vol. 46*, 48-61.

Castiglioni, I., Cremonesi, O., Gilardi, M. C., Bettinardi, V., Rizzo, G., Savi, A., Belloti, E., & Fazio, F. (1999). Scatter correction techniques in 3D PET: a Monte Carlo evaluation. *IEEE Trans. Nucl. Sci.*, *vol. 46*, 2053–2058.

Cheng, P., Kinahan, P. E., Comtat, C., Kim, S., Lartizen, C., & Lewellen, T. (April 15-18 2004). Effects of scan duration on lesion detectability in PET oncology imaging. *Biomedical Imaging: Nano to Macro*, *vol. 2*, 1432-1435.

Comtat, C., Kinahan, P. E., Defrise, M., Michel, C., Lartizen, C., & Townsend, D. W. (1999). Simulating Whole-Body PET Scanning with Rapid Analytical Methods. *Nuclear Science Symposium*, *vol. 3*, 1260-1264.

Daube-Witberspoon. Sim3D (Online). NIH(1994).

EGS (Online). http://www.slac.stanford.edu/, (1985).

Elston, B. (September 24 2009). *Introduction to ASIM 2.1.1: A PET Analytic Simulator*. Proceedings from Imaging Research Laboratory Scientific Retreat Conference Record, Seattle, WA.

EORTC (European Organization for Research and Treatment of Cancer) (Online). http://www.eortc.be/, (2011).

Furuie, S. S., Herman, G. T., Narayan, T. K., Kinahan, P. E., Karp, J. S., Lewitt, R. M., & Matej, S. (1994). A methodology for testing for statistically significant differences between fully 3D PET reconstruction algorithms. *Phys. Med. Biol.*, *vol. 39*, 341–354.

GATE: Geant4 Application for Tomographic Emission (Online). http://www-lphe.epfl.ch/GATE/, (2004).

GEANT (Online). http://geant4.web.cern.ch/geant4/.

Gu, S., Chakraborty, G., Champley, K., Alessio, A. M., Claridge, J., Rockne, R., Muzi, M., Krohn, K. A., Spence, A. M., Alvord, E. C., Anderson, A. R. A., Kinahan, P. E., & Swanson, K. R. (2011). Applying A Patient-Specific Bio-Mathematical Model of Glioma Growth to Develop Virtual [18F]-FMISO PET Images. *Mathematical Medicine & Biology*.

Harrison, R., Elston, B., Doot, R., Mankoff, D., Lewellen, T., & Kinahan, P. E. (2010). SNR Effects in Determining Change in PET SUVs in Response to Therapy.

Haynor, D. R., Kaplan, M. S., & Miyaoka, R. S. (1995). Multiwindow scatter correction techniques in single-photon imaging. *Med. Phys.*, *vol. 22*, 2015-2024.

Haynor, D. R., & Woods, S. D. (1989). Resampling estimates of precision in emission tomography. *IEEE Trans. Med. Im.*, *vol. 8*, 337-343.

Holdsworth, Houghton. (2002). Investigation of PET image reconstruction and data correction techniques with emphasis on an accelerated Monte Carlo simulation for correction and evaluation of PET.

Janeiro, L., Comtat, C., Lartizien, C., Kinahan, P. E., Defrise, M., Michel, C., Trébossen, R., & Almeida, P. (2006). Numerical Observer Studies Comparing FORE + AWOSEM, FORE + NECOSEM and NEC Based Fully 3-D OSEM for 3-D Whole-Body PET Imaging. *EEE Transactions on Nuclear Science*, *vol. 53*, 1194-1199.

Kinahan, P. E., Cheng, P., Alessio, A., & Lewellen, T. (2005). *A quantitative approach to a weight-based scanning protocol for PET oncology imaging*. Proceedings from IEEE Nucl. Sci. Symp. and Med. Imaging Conf., Puerto Rico.

Kinahan, P. E., Harrison, R., Elston, B., Doot, R., Lewellen, T., & Mankoff, D. (2011). Effects of noise, calibration, reconstruction and analysis methods on correctly determining change in PET SUVs.

Lahorte, P., Vandenberghe, S., & Van Laere, K. (2000). Assessing the Performance of SPM Analyses of Spect Neuroactivation Studies. *NeuroImage*, *vol. 12*, 757–764.

Lartizien, C., Kinahan, P. E., & Comtat, C. (2004). Volumetric Model and Human Observer Comparisons of Tumor Detection for Whole-Body PET. *Academic Radiology*, *vol. 11*, 637-648.

Lartizien, C., Kinahan, P. E., Swensson, R., Comtat, C., Lin, M., Villemagne, V., & Trébossen, R. (2003). Evaluating Image Reconstruction Methods for Tumour Detection in 3-Dimensional Whole-Body PET Oncology Imaging. *The Journal of Nuclear Medicine*, *vol. 44*, 276-290.

Lewellen, T. K., Harrison, R. L., & Vannoy, S. (1998). The SimSET program. In M. Ljungberg, S. E. Strand, & M. A. King (Eds.), *Monte Carlo Calculations in Nuclear Medicine* (pp. 77-92). Eds. Bristol: Institute of Physics Publishing.

Ljungberg, M., & Strand, S. E. (1989). A Monte Carlo Program Simulating Scintillation Camera Imaging. *Comp. Meth. Progr. Biomed.*, *vol. 29*, 257-272.

Ljungberg, M., Strand, S. E., & King, M. A. (1998). *Monte Carlo Calculations in Nuclear Medicine.* Bristol: Institute of Physics Publishing.

Marcinkowski, A., Layfield, D., Tgavalekos, N., & Venegas, J. G. (NOV 2005). Enhanced parameter estimation from noisy PET data: part II – Evaluation. *Academic Radiology*, *vol. 12*(11), 1448-1456.

Maroy, R., Boisgard, R., Comtat, C., Frouin, V., Cathier, P., Duchesnay, E., Dolle, F., E, N. P., Trébossen, R., & Tavitian, B. (2008). Segmentation of Rodent Whole-Body Dynamic PET Images: An Unsupervised Method Based on Voxel Dynamics. *IEEE Transactions on Medical Imaging*, *vol. 27*, 342-354.

MCNP. Los Alamos National Laboratory.,From: http://mcnp-green.lanl.gov/index.html.

Ollinger, J. M. (1996). Model-based scatter correction for fully 3D PET. *Physics in Medicine and Biology*, *vol. 41*(1), 153.

PENELOPE2005, A Code System for Monte-Carlo Simulation of Electron and Photon Transport (Online). http://www.nea.fr/abs/html/nea-1525.html.

PERCIST (PET Response Criteria In Solid Tumors). Siemens Healthcare Molecular Imaging.,From: http://www.medical.siemens.com, (2010).

PET-EGS (Online). http://www.slac.stanford.edu/.

Rowe, R., & Shubo, D. (Jul/Aug 1992). A pseudo-Poisson noise model for simulation of positron emission projection data. *Medical Physics*, *vol. 19*(4).

Sempau, J., Fernandez-Varea, J. M., Acosta, E., & Salvat, F. (2003). Experimental benchmarks of the Monte Carlo code PENELOPE. *Nuclear Instruments and Methods*, *vol. 207*, 107-123.

SIMIND (Online). http://www.radfys.lu.se/simind/.

SimSET: A Simulation System for Emission Tomography (Online). http://depts.washington.edu/simset/html/simset_main.html.

STIR: Software for Tomographic Image Reconstruction (Online). Hammersmith Imanet.,From: http://stir.sourceforge.net/.

Tai, Y. C., Wu, H., & Janecek, M. (2006). Initial Study of an Asymmetric PET System Dedicated to Breast Cancer Imaging. *IEEE Trans. Nucl. Sci.*, *vol. 53*(1), 121-126.

Thompson, C. J., Moreno-Cantu, J., & Picard, Y. (1992). PETSIM: Monte Carlo simulation of all sensitivity and resolution parameters of cylindrical positron imaging systems. *Phys. Med. Biol.*, *vol. 37*(3), 731-749.

Ward, T., Fleming, J. S., Hoffmann, S. M., & Kemp, P. M. (2005). Simulation of realistic abnormal SPECT brain perfusion images: application in semi-quantitative analysis. *Phys. Med. Biol.*, *vol. 50*, 5323-5338.

Watson, C. C. (Aug 2000). New, faster, image-based scatter correction for 3D PET. *IEEE Transactions on Nuclear Science*, *vol. 47*(4), 1587-1594.

Wollenweber, S. D. (Jun 2002). Parameterization of a model-based 3-D PET scatter correction. *IEEE Transactions on Nuclear Science*, *vol. 49*(3), 722-727.